Front. Phys. 11(4), 115202 (2016)
DOI 10.1007/s11467-016-0563-8

RESEARCH ARTICLE

Effect of pulse slippage on density transition-based resonant third-harmonic generation of short-pulse laser in plasma

Vishal Thakur, Niti Kant[†]

Department of Physics, Lovely Professional University, Phagwara -144411, Punjab, India

Corresponding author. E-mail: [†]*nitikant@yahoo.com*

Received June 26, 2015; accepted October 6, 2015

The resonant third-harmonic generation of a self-focusing laser in plasma with a density transition was investigated. Because of self-focusing of the fundamental laser pulse, a transverse intensity gradient was created, which generated a plasma wave at the fundamental wave frequency. Phase matching was satisfied by using a Wiggler magnetic field, which provided additional angular momentum to the third-harmonic photon to make the process resonant. An enhancement was observed in the resonant third-harmonic generation of an intense short-pulse laser in plasma embedded with a magnetic Wiggler with a density transition. A plasma density ramp played an important role in the self-focusing, enhancing the third-harmonic generation in plasma. We also examined the effect of the Wiggler magnetic field on the pulse slippage of the third-harmonic pulse in plasma. The pulse slippage was due to the group-velocity mismatch between the fundamental and third-harmonic pulses.

Keywords short pulse laser, pulse slippage, third harmonic generation, plasma

PACS numbers 52.35.Mw, 52.38.Dx

1 Introduction

The interaction of high-power laser beams with plasmas and semiconductors has drawn interest in the past few decades, as it plays a major role in the study of various nonlinear phenomena [1–9]. Harmonic generation during high-power laser interactions with plasmas is one of the important nonlinear phenomena observed under different conditions [10, 11]. Third-harmonic generation is a very useful technique that converts the coherent output of infrared lasers to shorter wavelengths in the near-UV region, which makes intense laser filaments useful for remote-sensing applications [12].

The spectrum of the generated radiation depends strongly on the structure of the atomic levels. Theberge *et al.* experimentally and theoretically examined the third-harmonic generation in air during the filamentation of a powerful femtosecond laser pulse [13]. They found that the third-harmonic beam pattern exhibited a central spot on the propagation axis at low pump energy and was surrounded by bright third-harmonic conical emissions at higher pump energy. Akozbek *et al.* [14] observed that during the propagation of an ultrashort high power laser pulse in air, a third harmonic was generated, which maintained its energy and intensity over a distance far longer than the characteristic coherence length. A nonlinear theory for the harmonic generation of a finite spot-size laser was developed by Sprangle *et al.* [15–17]. They used it to describe relativistic optical guiding, coherent harmonic radiation production, and nonlinear plasma Wakefield generation. They suggested that these phenomena may be important in laser-driven plasma accelerators, X-ray sources, and fusion schemes. However, their treatment was limited to preformed plasma. An analytical model for the efficiency of third-harmonic generation from high-density inhomogeneous plasma produced by the laser irradiation of a thin metallic film was developed by Kaur and Sharma [18]. They observed that a laser propagating through plasma suffers reflection from the critical layer and creates a density ripple in the under-dense region, which helps the phase matching for the resonant generation of the third harmonic.

Efficient third-harmonic generation is required for various applications and can be obtained by satisfying the phase-matching condition. Thus, the phase-matching condition is important for third-harmonic generation, and various schemes have been proposed by many researchers to satisfy it. Wiggler magnetic fields play an important role in compensating the momentum mismatch between the fundamental and second harmonic [19, 3]. Parashar and Pandey [3] observed that when a Wiggler magnetic field was present in the system, the $\boldsymbol{V} \times \boldsymbol{B}$ force on the electrons produced a transverse second-harmonic current at $2\omega_1$ and $(2k_1 + k_0)\hat{z}$, inducing second-harmonic electromagnetic radiation. Kant and Sharma [20] examined the effect of the pulse slippage on the second-harmonic generation in plasma. The group velocity of the second-harmonic wave was found to be greater than that of the pump wave, causing the second-harmonic wave to slip out of the main pulse. The resonant third-harmonic generation of a short-pulse laser in plasma in the presence of a Wiggler magnetic field was proposed by Rajput *et al.* [21]. The generation of a second-harmonic wave by a Gaussian laser beam in plasma in the presence of a Wiggler magnetic field was reported by Kant *et al.* [22]. They observed an enhancement in the second-harmonic generation caused by the self-focusing of the fundamental pulse. The strong enhancement in the self-focusing of the fundamental laser pulse was caused by the introduction of an upward plasma density ramp, whereby the laser pulse attained a minimum spot size and propagated up by several Rayleigh lengths without divergence.

An analytical formalism of the resonant third-harmonic generation due to an intense short-pulse laser in rippled density plasma was developed by Liu and Tripathi [23]. The third harmonic is produced through ponderomotive force-induced second-harmonic density oscillations and the quiver velocity of the electron at the fundamental frequency. A density ripple can also be used to satisfy the phase-matching condition to make the process of harmonic generation resonant. A paraxial theory of third-harmonic generation by a finite spot-size laser in a tunnel with ionizing gas was developed by Verma and Sharma [24]. They observed that the laser, with an intensity close to the tunnel ionization threshold, created plasma whose density increased in a stepwise manner in every half wave period, yielding a strong second-harmonic component in the electron density. The electron density at the second harmonic beats oscillated with the oscillatory velocity at the fundamental frequency to produce a nonlinear current, driving the third-harmonic generation. Third-harmonic generation in collisional plasma by a Gaussian electromagnetic beam was investigated by Sodha *et al.* [25]. They found that the self-focusing of the main beam enhanced the power of the harmonic output by approximately three orders of magnitude in a typical paraxial-ray approximation. The application of Wiggler magnetic field is an important technique for satisfying the phase-matching condition.

In the present paper, we propose a scheme to introduce a density ramp profile for plasma, which plays a crucial role in strengthening the self-focusing and enhancing the third-harmonic generation in plasma. We consider the plasma density as a function of the propagation distance. The dependence of the plasma density on the third-harmonic generation was examined. As the plasma density ramp was introduced, the fundamental laser beam propagated to a longer distance without divergence. Thus, the plasma density ramp played a key role in the enhancement of the self-focusing. The Wiggler magnetic field provided additional angular momentum to the third-harmonic photon to compensate for the mismatch. The group velocity of the third-harmonic pulse was greater than that of the pump pulse; hence, the third-harmonic pulse slipped out of the domain of the pump pulse. Thus, the effect of the pulse slippage on the third-harmonic generation was demonstrated. The Wiggler magnetic field also supported the third-harmonic generation.

In Section 2, we describe the variation of the normalized amplitude of the third-harmonic wave A_3/A_0 with respect to the normalized propagation distance z'. Our numerical results are discussed in Section 3, and our conclusions are presented in Section 4.

2 Theoretical considerations

Consider the propagation of a Gaussian short-pulse laser beam in a preformed plasma channel with an upward plasma density ramp along the z-direction in the presence of a Wiggler magnetic field $\boldsymbol{B}_W$. The field of the laser beam and the applied Wiggler magnetic field can be written as

$$\boldsymbol{E}_1 = \hat{x} A_1(z,t) \exp[-\mathrm{i}(\omega_1 t - k_1 z)], \tag{1}$$

$$\boldsymbol{B}_1 = \frac{c\boldsymbol{k}_1 \times \boldsymbol{E}_1}{\omega_1}, \tag{1a}$$

$$\boldsymbol{B}_W = \hat{y} B_0 \exp(\mathrm{i}k_0 z), \tag{1b}$$

where $A_1(z,t) = F(z - v_{g1}t)$ is the amplitude of the fundamental laser pulse inside the plasma, and $v_{g1} = c(1 - \omega_p^2/\omega_1^2)^{1/2}$ is the group velocity of the fundamental pulse. The laser pump and third-harmonic electromagnetic wave obey the linear-dispersion relation, i.e., $k_1^2 \approx (\omega_1^2/c^2)(1 - \omega_P^2/\omega_1^2)$, where k_1 and ω_1 are the wave number and angular frequency, respectively, of the fundamental laser beam, and ω_p is the plasma frequency. The wave vector k_1 increases more than linearly with the fundamental frequency ω_1; hence, $k_3 > 3k_1$. A change in momentum can be provided to the third-harmonic photon by the Wiggler magnetic field when $k_3 = 3k_1+k_0$; the Wiggler wave number k_0 required for the phase matching can be obtained as $k_0 = (3\omega_1/c)[(1-\omega_P^2/9\omega_1^2)^{1/2} - (1-\omega_P^2/\omega_1^2)^{1/2}]$, where $\omega_P = (4\pi\ n(z')\ e^2/m)^{1/2}$ is the plasma frequency. The upward plasma density ramp profile is given as $n\,(z') = n_0 \tan(z'/d)$, where $z' = z/\xi_0$. Here, τ is the laser pulse length, c is the velocity of light in vacuum, n_0 is the initial electron density, d is an adjustable constant, and e and m are the charge and rest mass of the electron, respectively. Furthermore, k_1 may be written as $k_1 = \sqrt{\omega_1^2 - \omega_{p0}^2 \tan(z'/d)}$.

2.1 Plasma-wave generation

To analyze the generation of the electron plasma wave, we consider the following set of equations:

$$\frac{\partial N}{\partial t} + \boldsymbol{\nabla}.(N\boldsymbol{V}) = 0, \tag{2}$$

$$m[\frac{\partial \boldsymbol{V}}{\partial t} + (\boldsymbol{V}.\boldsymbol{\nabla})\boldsymbol{V}] = -e\boldsymbol{E} - \frac{e}{c}\boldsymbol{V}\times\boldsymbol{B} \\ -2\Gamma_e m\boldsymbol{V} - \frac{3k_0T_e}{N}\boldsymbol{\nabla}N, \tag{3}$$

$$\boldsymbol{\nabla}\cdot\boldsymbol{E} = -4\pi e N, \tag{4}$$

where N is the total electron density, E is the sum of the electric vectors of the laser beam and the self-consistent field, and V is the sum of the drift velocities of the electron in the laser field and self-consistent field. Using Eqs. (2), (3), and (4), we obtain the following equation for N:

$$\frac{\partial^2 N}{\partial t^2} - V_{th}^2\boldsymbol{\nabla}^2 N + 2\Gamma_e\frac{\partial N}{\partial t} - \frac{e}{m}\boldsymbol{\nabla}\cdot(N\boldsymbol{E}) \\ = \boldsymbol{\nabla}[\frac{N}{2}\boldsymbol{\nabla}(BVV^*) - \boldsymbol{V}\frac{\partial N}{\partial t}], \tag{5}$$

where $V_{th}^2 = 3k_0T_e/m$ is the thermal velocity of the electron, and $2\Gamma_e$ is the Landau damping factor.

2.2 Third-harmonic generation

The wave equation for the third-harmonic field E_3 is formulated using Maxwell's equations:

$$\nabla^2\boldsymbol{E}_3 = \frac{4\pi}{c^2}\frac{\partial \boldsymbol{J}_3}{\partial t} + \frac{1}{c^2}\frac{\partial^2\boldsymbol{E}_3}{\partial t^2}, \tag{6}$$

where $\boldsymbol{J}_3 = \boldsymbol{J}_3^L + \boldsymbol{J}_3^{NL}$, and $\boldsymbol{J}_3^L$ is the linear current density due to the self-consistent field $\boldsymbol{E}_3$; additionally, $\boldsymbol{J}_3^L = -n_0e\boldsymbol{v}_3^L$, where $\boldsymbol{v}_3^L$ is governed by the equation of motion $\partial\boldsymbol{v}_3^L/\partial t = -e\boldsymbol{E}_3/m$, giving

$$\frac{\partial \boldsymbol{J}_3}{\partial t} = \frac{n_0e^2\boldsymbol{E}_3}{m}. \tag{7}$$

According to Rajput *et al.* [21], the nonlinear current density at the third harmonic can be written as

$$\boldsymbol{J}_3^{NL} = -\frac{n_0e^5B_wk_1E_1^3}{16m^4c\omega_1^5(\omega_1+\mathrm{i}v)}(\frac{5k_1}{18\omega_1} + \frac{k_1+k_0}{\omega_1+\mathrm{i}v})\hat{x}.$$

The solution of Eq. (6) can be assumed as

$$E_3 = xA_3\,(z,t)\exp[-\mathrm{i}\,(3\omega_1t - k_3z)], \tag{8}$$

where $A_3\,(z,t)$ is the complex amplitude of the electric field of the third-harmonic wave, given as $A_3(z,t) = [F(z - v_{g3}t)]$. By solving Eq. (6), we obtain

$$\frac{\partial A_3}{\partial z} + \frac{1}{v_{g3}}\frac{\partial A_3}{\partial t} = \alpha_3A_1^3, \tag{9}$$

where $A_1^3 = [F(z - v_{g1}t)]^3$ and $v_{g3} = c(1-\omega_p^2/9\omega_1^2)^{1/2}$. Moreover,

$$\alpha_3 = \frac{3\omega_p^2e^3B_wk_1}{32m^3\omega_1^4ck_3}(\frac{23k_1}{18} + k_0), \tag{10}$$

or

$$\alpha_3 = \frac{3(\frac{4\pi\ n(z')\ e^2}{m})e^3B_wk_1}{32m^3\omega_1^4ck_3}(\frac{23k_1}{18} + k_0), \tag{11}$$

or

$$\alpha_3 = \frac{3(\frac{4\pi\ n_0\tan\frac{z'}{d}\ e^2}{m})e^3B_wk_1}{32m^3\omega_1^4ck_3}(\frac{23k_1}{18} + k_0). \tag{12}$$

Now, we specify the temporal profile of laser pulse to be Gaussian, $F(z - v_{g1}t) = A_0\exp(-(z - v_{g1}t)^2/\tau^2v_{g1}^2)$. Introducing a new set of variables $z - v_{g1}t = \xi$, and $z = \eta$, we can write $\partial/\partial z = \partial/\partial\xi + \partial/\partial\eta$, $\partial/\partial t = -v_{g1}\partial/\partial\xi$, and Eq. (9) can be written as

$$\beta\frac{\partial A_3}{\partial\xi} + \frac{\partial A_3}{\partial\eta} = \alpha_3A_0^3\exp\left(\frac{\xi^2}{\xi_0^2}\right), \tag{13}$$

where $\beta = (1 - v_{g1}/v_{g3})$. The complementary solution of Eq. (13) is $A_3 = -(\alpha_3A_0^3/\beta)f(\xi - \beta\eta)$while the particular integral is $A_3 = (\alpha_3A_0^3/\beta)f(\xi)$ where $f(\xi) = \int_{-\infty}^{\xi}\exp(-\xi^2/\xi_0^2)\mathrm{d}\xi$. Hence, the complete solution of Eq. (13) can be written as

$$A_3 = \frac{\alpha_3\xi_0A_0^3\sqrt{\pi}}{2\beta}[erf(\frac{\xi}{\xi_0}) - erf(\frac{\xi - \beta\eta}{\xi_0})], \tag{14}$$

where $erf(\psi)$ is the error function of the argument ψ. Using Eqs. (12) and (14), the ratio of the amplitude of the third harmonic to that of the pump pulse can be obtained as

$$\left|\frac{A_3}{A_0}\right| = \left| \begin{array}{c} \dfrac{3\omega_{p0}^2 e^3 A_0^2 B_w z' \sqrt{\pi} \tan\dfrac{z'}{d}\left(1-h^2\tan\dfrac{z'}{d}\right)^{\frac{1}{2}}}{64\left[1-\dfrac{\left(1-h^2\tan\dfrac{z'}{d}\right)^{\frac{1}{2}}}{\left(1-\dfrac{h^2}{9}\tan\dfrac{z'}{d}\right)^{\frac{1}{2}}}\right]\omega_1^4 m^3 c^4 \beta\left[3\left(1-h^2\tan\dfrac{z'}{d}\right)^{\frac{1}{2}}+k\right]}\left[\dfrac{23}{18}\left(1-h^2\tan\dfrac{z'}{d}\right)^{\frac{1}{2}}+k\right] \\ \left[erf\left(z'-t'\left(1-h^2\tan\dfrac{z'}{d}\right)^{\frac{1}{2}}\right)-erf\left\{\left(1-\left[1-\dfrac{\left(1-h^2\tan\dfrac{z'}{d}\right)^{\frac{1}{2}}}{\left(1-\dfrac{h^2}{9}\tan\dfrac{z'}{d}\right)^{\frac{1}{2}}}\right]\right)z'-t'\left(1-h^2\tan\dfrac{z'}{d}\right)^{\frac{1}{2}}\right\}\right] \end{array} \right|, \quad (15)$$

where $t' = v_{g1}t/\xi_0$ is a dimensionless quantity. Eq. (15) describes the variation of the normalized amplitude of the third-harmonic wave A_3/A_0 with respect to the normalized propagation distance z'. The efficiency of the third-harmonic generation is given as $\eta = |A_3/A_0|^2$.

3 Result and discussion

We solved Eq. (15) numerically for the normalized amplitude of the third-harmonic wave by applying the boundary conditions corresponding to an initial plane wave front at $z' = 0$. In a typical case of plasma irradiated by a 1.06 μm Nd:YAG laser with a pulse duration of 2.5 ps and a laser spot size of 45 μm, under a Wiggler magnetic field of $B_W = 10$ T, the Wiggler period was ∼0.2 cm, which is experimentally feasible. The group-velocity mismatch between the fundamental and third-harmonic pulses was significant in high-density plasma and increased with the plasma density. The group velocity of the third harmonic was greater than that of the pump wave; hence, the third-harmonic pulse slipped out of the domain of the pump pulse. Figure 1 shows the variation of the normalized plasma density with respect to the normalized propagation distance $z' = z/\xi_0$ for d =4, 6, and 8. Clearly, for $d = 8$, the plasma density n_e/n_0 varied slowly with respect to the propagation distance z'. Compared with the cases of $d = 4$ and 6, the slowly varying plasma density may have enhanced the third-harmonic generation by increasing the intensity in the focal region [26–29]. Figure 2 shows the variation of the normalized third-harmonic amplitude with respect to the propagation distance for different values of t for (a) $\omega_{p0}/\omega_1 = 0.4$, (b) $\omega_{p0}/\omega_1 = 0.6$, and (c) $\omega_{p0}/\omega_1 = 0.8$. The other parameters are $eA_0/(m\omega_1 c) = 2$, $eB_w/(m\omega_1 c) = 0.005$, and $d = 8$. Figure 2 clearly shows that a third-harmonic pulse with a small amplitude was generated in the domain of the fundamental laser pulse at $t = 2$. The normalized amplitude of the fundamental laser pulse is denoted by A_1/A_0. As time passes, the amplitude of the third-harmonic pulse increased, and the pulse slipped out of the domain of the fundamental laser pulse. This is because of the phase mismatch that occurred between the fundamental and third-harmonic pulses because the group velocity of the third-harmonic wave was greater than that of fundamental wave. In Fig. 2, the effect of the pulse slippage is observed, and the amplitude of the third harmonic is shown to increase with time. Similar results were reported by Aggarwal *et al.* [30]. They observed an enhancement in the second-harmonic generation with the effect of a Wiggler magnetic field in clusters. This is because the group velocity of the second harmonic is greater than that of the fundamental pulse, yielding the pulse slippage of the second-harmonic wave. A Wiggler strength of ⩾ 10 kG is needed to achieve a high efficiency of third-harmonic generation. Vij *et al.* [31] examined the effect of the pulse slippage on the resonant third-harmonic generation in clusters in the presence of a density ripple. They observed that the third-harmonic amplitude increased with time. We obtained similar results, as shown in Fig. 2.

Figure 3 shows the variation of the normalized third-harmonic amplitude with respect to the propagation distance for different values of n_0: 1.58×10^{19} cm^{-3}, 3.57×10^{19} cm^{-3}, and 6.35×10^{19} cm^{-3}. The other parameters are the same as in Fig. 2. A sharp increase in the normalized third-harmonic amplitude is observed for $n_0 = 6.35 \times 10^{19}$ cm^{-3} at $z' = 3$. Therefore, the third-harmonic

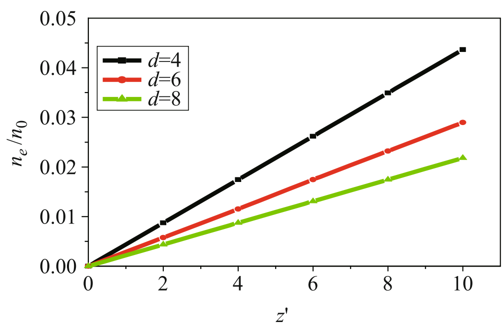

Fig. 1 Variation of the normalized plasma density with respect to the normalized propagation distance z' for d = 4, 6, and 8.

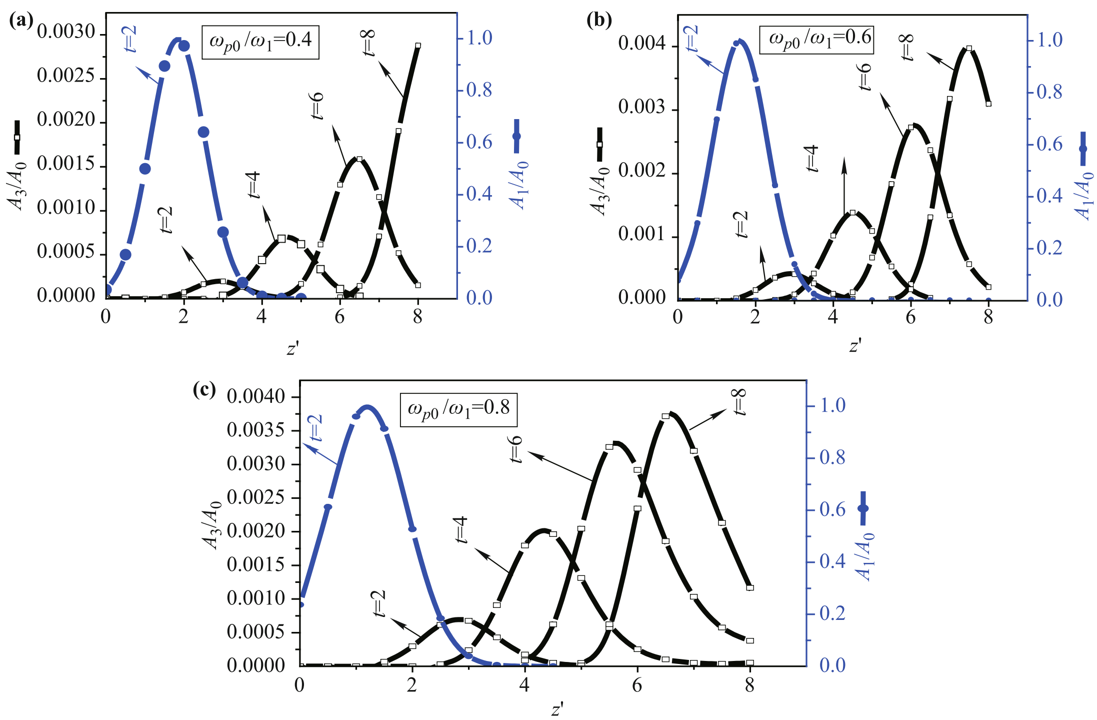

Fig. 2 Variation of the normalized amplitude with respect to the normalized propagation distance z' for different values of different values of t for **(a)** $\omega_{p0}/\omega_1 = 0.4$, **(b)** $\omega_{p0}/\omega_1 = 0.6$, **(c)** $\omega_{p0}/\omega_1 = 0.8$. The other parameters are $eA_0/(m\omega_1 c) = 2$, $eB_w/(m\omega_1 c) = 0.005$, and $d = 8$.

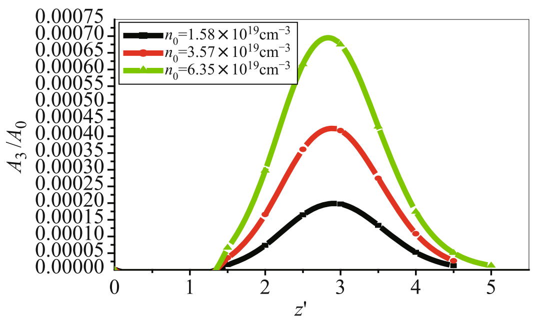

Fig. 3 Variation of the normalized third-harmonic amplitude with respect to the normalized propagation distance z' for $t = 2$, $eA_0/(m\omega_1 c) = 2$, $eB_w/(m\omega_1 c) = 0.005$, and $d = 8$.

generation process was more pronounced in high density plasma, as reported by Ganeev*et al.* [32], who stated that the plasma electron density plays a crucial role in enhancing the phase mismatch between the pump and harmonic radiation to make the process resonant. Figure 4 shows the variation of the normalized third-harmonic amplitude with respect to the propagation distance for different values of the normalized fundamental intensity parameter: $eA_0/(\omega_1 mc) = 2$, 4, and 6 (corresponding intensities are $I_0 \approx 5.4 \times 10^{13}$, 2.1×10^{14}, and 4.8×10^{14} W/cm^2, respectively). The other parameters are the same as in Fig. 2. Figure 4 clearly shows that as the intensity of the fundamental laser beam increased, the efficiency of the third harmonic increased. Aggarwal *et al.* reported an enhancement in the second-harmonic generation in clusters with the increase of the intensity of the fundamental beam [30]. They suggested the following physical reason for this: with the increase of the laser intensity, the strength of the ponderomotive force, as well as the initial ionization of atoms in the clusters, increased. Figure 5 shows the variation of normalized third-harmonic amplitude with respect to the propagation distance for different normalized values of the magnetic field: $eB_w/(\omega_1 mc) = 0.0005$, 0.001, and 0.005. The other parameters are the same as in Fig. 2. The normalized third-harmonic amplitude increased with the Wiggler magnetic field strength. The Wiggler magnetic field played a crucial role in the enhancement of the intensity

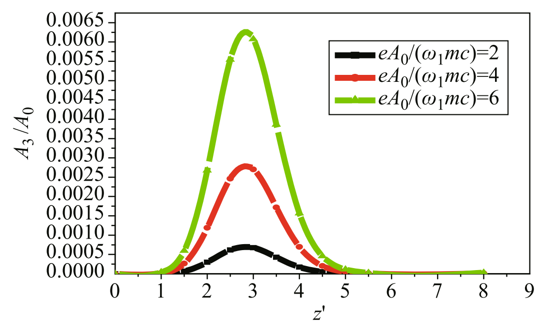

Fig. 4 Variation of the normalized third-harmonic amplitude with respect to the normalized propagation distance z' for $t = 2$, $\omega_{p0}/\omega_1 = 0.8$, $eB_w/(m\omega_1 c) = 0.005$, and $d = 8$.

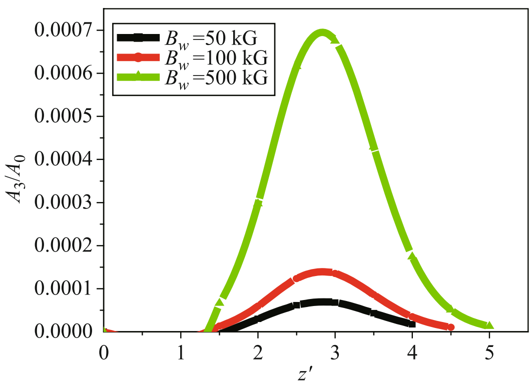

Fig. 5 Variation of the normalized third-harmonic amplitude with respect to the normalized propagation distance z' for $t = 2$, $\omega_{p0}/\omega_1 = 0.8$, $eA_0/(m\omega_1 c) = 2$, and $d = 8$.

of third-harmonic generation. We also observed the variation of the efficiency of the third-harmonic generation with respect to the normalized propagation distance and the Wiggler wave number, and the results are plotted in Figs. 6 and 7. An enhancement in the efficiency of the third harmonic was observed for the optimum values of the Wiggler magnetic field. In Fig. 6, at $z' = 3$, as the intensity of the fundamental laser beam increased, the efficiency of the third harmonic increased. The efficiency of third-harmonic generation increased greatly with the

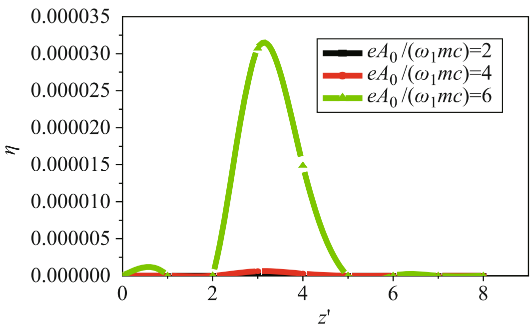

Fig. 6 Variation of the normalized third-harmonic efficiency with respect to the normalized propagation distance z' for $t = 2$, $\omega_{p0}/\omega_1 = 0.8$, $eB_w/(m\omega_1 c) = 0.005$, and $d = 8$.

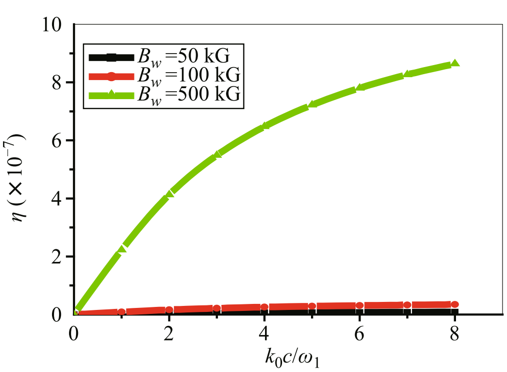

Fig. 7 Variation of the normalized third-harmonic efficiency η with respect to the normalized Wiggler wave number k_0c/ω_1 for $t = 2$, $\omega_{p0}/\omega_1 = 0.8$, $eA_0/(m\omega_1 c) = 2$, and $d = 8$.

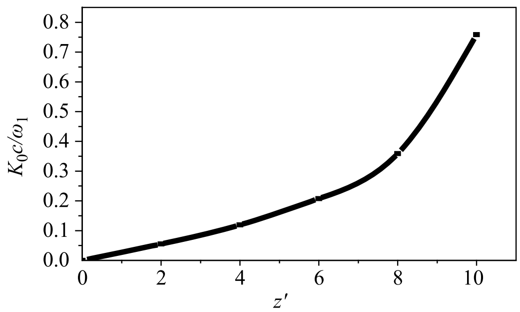

Fig. 8 Variation of the normalized Wiggler wave number k_0c/ω_1 with respect to the normalized propagation distance z' for $\omega_{p0}/\omega_1 = 0.4$ and $d = 8$.

Wiggler magnetic field because of the self-focusing of the fundamental laser beam, as shown in Fig. 7. The dynamics of the oscillating electrons were changed by the Lorentz force, which modified the plasma wave, significantly affecting the third harmonic. The efficiency of the third-harmonic generation increased with the strength of the Wiggler magnetic field. Figure 8 shows the variation of the normalized Wiggler wave number with respect to the normalized propagation distance $z' = z/\xi_0$ for $\omega_{p0}/\omega_1 = 0.4$. Under the influence of the Wiggler magnetic field, the Wiggler wave number increased with the propagation distance.

4 Conclusion

A slowly varying plasma density ramp is crucial for laser-plasma interaction. This is because the density ramp is important for making strengthening the self-focusing of short laser pulses, which enhances the harmonic generation [22, 25]. The group-velocity mismatch between the fundamental laser pulse and the third-harmonic pulse is significant in high-density plasma. The wiggler magnetic field also plays a crucial role, providing additional angular momentum to the third-harmonic photon to make the process resonant, yielding efficient third-harmonic generation. Rajput *et al.* [21] reported that the third-harmonic efficiency increases linearly with the normalized fundamental intensity and is saturated for a high-intensity fundamental laser beam. This is because at a high intensity, there is a strong relativistic effect, and the large ponderomotive force of the laser expels the plasma electrons from the axis of laser propagation. Thus, the plasma frequency on the axis is lower, and less energy is converted into the third harmonic. However, in the present study, under a plasma density transition, the third-harmonic efficiency increased linearly with respect to the normalized fundamental intensity. The present analysis may be useful for the study of laser-induced fusion, in which third-harmonic generation plays an important role. We also observed that the efficiency of the third-harmonic generation increased with the fundamental intensity and strength of the Wiggler magnetic field.

Acknowledgements This work was supported by a financial grant from CSIR, New Delhi, India, under Project No. 03 (1277 /13/EMR -11).

References

1. J. K. Sharma and J. Parashar, Parametric instability of a lower hybrid wave in a dusty plasma, *Indian J. Pure & Appl. Phys.* 41, 290 (2003)
2. J. K. Sharma, J. Parashar, and A. S. Mehta, Relativistic stimulated Raman scattering in a plasma channel, *Indian J. Pure & Appl. Phys.* 41, 73 (2003)
3. J. Parasher and H. D. Pandey, Second-harmonic generation of laser radiation in a plasma with a density ripple, *IEEE Trans. Plasma Sci.* 20(6), 996 (1992)
4. J. Parashar and A. K. Sharma, Second harmonic generation by an obliquely incident laser on a vacuum plasma interface, *Europhys. Lett.* 41(4), 389 (1998)
5. T. K. Pramanik and D. P. Bhattacharya, Harmonic generation in semiconductors in the presence of deep repulsive traps, *Solid State Commun.* 74(6), 539 (1990)
6. N. Kant, D. N. Gupta, and H. Suk, Resonant third-harmonic generation of a short-pulse laser from electron-hole plasmas, *Phys. Plasmas* 19(1), 013101 (2012)
7. J. F. Han, D. N. Gao, H. Zhang, X. Y. Wang, and W. S. Duan, Effects of the dust size distribution in one-dimensional quantum dusty plasma, *Front. Phys.* 10(5), 105201 (2015)
8. H. H. Zhang, D. C. Mao, and Y. N. Wang, Current neutralization and plasma polarization for intense ion beams propagating through magnetized background plasmas in a two-dimensional slab approximation, *Front. Phys.* 9(2), 226 (2014)
9. X. G. Wang and Q. B. Luan, Low frequency whistler waves excited in fast magnetic reconnection processes, *Front. Phys.* 8(5), 585 (2013)
10. V. Malka, A. Modena, Z. Najmudin, A. E. Dangor, C. E. Clayton, K. A. Marsh, C. Joshi, C. Danson, D. Neely, and F. N. Walsh, Second harmonic generation and its interaction with relativistic plasma waves driven by forward Raman instability in underdense plasmas, *Plasma Phys.* 4(4), 1127 (1997)
11. E. Esarey, A. Ting, P. Sprangle, D. Umstadter, and X. Liu, Nonlinear analysis of relativistic harmonic generation by intense lasers in plasmas, *IEEE Trans. Plasma Sci.* 21(1), 95 (1993)
12. A. Kuditcher, B. G. Hoover, M. P. Hehlen, E. N. Leith, S. C. Rand, and M. P. Shih, Ultrafast, cross-correlated harmonic imaging through scattering media, *Appl. Opt.* 40(1), 45 (2001)
13. F. Théberge, N. Aközbek, W. Liu, J. F. Gravel, and S. L. Chin, Third harmonic beam profile generated in atmospheric air using femtosecond laser pulses, *Opt. Commun.* 245(1–6), 399 (2005)
14. N. Aközbek, A. Iwasaki, A. Becker, M. Scalora, S. L. Chin, and C. M. Bowden, Third harmonic generation and self-channeling in air using high-power femtosecond laser pulses, *Phys. Rev. Lett.* 89(14), 143901 (2002)
15. P. Sprangle, E. Esarey, and A. Ting, Nonlinear interaction of intense laser pulses in plasmas, *Phys. Rev. Lett.* 41, 4463 (1990)
16. E. Esarey and P. Sprangle, Generation of stimulated backscattered harmonic radiation from intense-laser interactions with beams and plasmas, *Phys. Rev. A* 45(8), 5872 (1992)
17. P. Sprangle, E. Esarey, and A. Ting, Nonlinear theory of intense laser-plasma interactions, *Phys. Rev. Lett.* 64(17), 2011 (1990)
18. S. Kaur and A. K. Sharma, Resonant third harmonic generation in a laser produced thin foil plasma, *Phys. Plasmas* 15(10), 102705 (2008)
19. N. Kant and V. Thakur, Enhanced resonant second harmonic generation in plasma based on density transition, *Nukleonika.* 60(2), 355 (2015)
20. N. Kant and A. K. Sharma, Effects of pulse slippage on resonant second harmonic generation of a short pulse laser in a plasma., *J. Phys. D Appl. Phys.* 37(7), 998 (2004)
21. J. Rajput, N. Kant, H. Singh, and V. Nanda, Resonant third harmonic generation of a short pulse laser in plasma by applying a wiggler magnetic field, *Opt. Commun.* 282(23), 4614 (2009)
22. N. Kant, D. N. Gupta, and H. Suk, Generation of second harmonic radiations of a self-focusing laser from plasma with density-transition, *Phys. Lett. A* 375(35), 3134 (2011)
23. C. S. Liu and V. K. Tripathi, Third harmonic generation of a short pulse laser in a plasma density ripple created by a machining beam, *Phys. Plasmas* 15(2), 023106 (2008)
24. U. Verma and A. K. Sharma, Effect of laser self-defocusing on third harmonic generation in a tunnel ionizing gas, *Phys. Plasmas* 16(1), 013101 (2009)
25. M. S. Sodha, R. K. Khanna, and V. K. Tripathi, Nonlinear third-harmonic generation in a plasma by a Gaussian electromagnetic beam: Effect of self-focusing, *Phys. Rev. A* 12(1), 219 (1975)
26. N. Kant, M. A. Wani, and A. Kumar, Self-focusing of Hermite-Gaussian laser beams in Plasma under plasma density ramp, *Opt. Commun.* 285(21–22), 4483 (2012)
27. V. Nanda, N. Kant, and M. A. Wani, Self-focusing of a Hermite-cosh Gaussian laser beam in a magnetoplasma with ramp density profile, *Phys. Plasmas* 20(11), 113109 (2013)

28. V. Nanda and N. Kant, Enhanced relativistic self-focusing of Hermite-cosh-Gaussian (HChG) laser beam in plasma under density transition, *Phys. Plasmas* 21(4), 042101 (2014)

29. V. Nanda and N. Kant, Strong Self-Focusing of a cosh-Gaussian Laser Beam in collisionless magneto-plasma under plasma density ramp, *Phys. Plasmas* 21(7), 072111 (2014)

30. M. Aggarwal, S. Vij, and N. Kant, Wiggler magnetic field assisted second harmonic generation in clusters, *Eur. Phys. J.* 69, 149 (2015)

31. S. Vij, N. Kant, and M. Aggarwal, Resonant third harmonic generation in clusters with density ripple: Effect of pulse slippage, *Laser and Part. Beams* 1, 1 (2016)

32. R. A. Ganeev, G. S. Boltaev, R. I. Tugushev, T. Usmanov, M. Baba, and H. Kuroda, Third harmonic generation in plasma plumes using picosecond and femtosecond laser pulses, *J. Opt.* 12(5), 055202 (2010)